

VHF coherent radar signals from the *E* region ionosphere and the relationship to electron drift velocity and ion acoustic velocity

E. Nielsen

Max-Planck-Institut für Aeronomie, Katlenburg-Lindau, Germany

C. F. del Pozo

Communications Research Centre, Faculty of Applied Sciences, Lancaster University, Lancaster, UK

P. J. S. Williams

Adran Ffiseg, Prifysgol Cymru, Aberystwyth, UK

Received 12 January 2001; revised 3 July 2001; accepted 12 July 2001; published 22 January 2002.

[1] The Scandinavian Twin Auroral Radar Experiment (STARE) coherent radar system measures the Doppler shifts caused by ~ 1 m plasma waves in the high-latitude *E* region ionosphere. These Doppler velocities are here related to the electron drift velocity and ion acoustic velocity derived from measurements with the incoherent radar system European Incoherent Scatter (EISCAT). The Doppler velocity is limited in magnitude to near the ion acoustic velocity in the plasma. For large flow angles θ , i.e., the angle between the radar line of sight and the electron drift velocity, the Doppler shifts are equal to the component of the electron drift velocity on the line of sight. For $\theta \sim 40^\circ$ the Doppler velocity is equal to the ion acoustic velocity at 105-km altitude, and for decreasing flow angle the Doppler velocity increases. For $0^\circ < \theta < 60^\circ$ the variation with flow angle can be described as $\cos^\alpha \theta$, where the α decreases from 0.8 to 0.2 with an increase in drift speed from ~ 400 to 1600 ms^{-1} . The ratio of the line-of-sight velocity for $\theta \sim 0^\circ$ to the ion acoustic velocity decreases from 1.2 at low velocities to 1.05 at large velocities. The systematic variations of the Doppler shifts with drift speed and flow angle make it possible, in principle, to recover the electron velocity from the coherent radar measurements. The observations are used to illustrate how well the recovery is possible in practice. *INDEX TERMS*: 2407 Ionosphere: Auroral ionosphere (2704), 2411 Ionosphere: Electric fields (2712), 2471 Ionosphere: Plasma waves and instabilities, 2494 Ionosphere: Instruments and techniques

1. Introduction

[2] At high latitudes, strong electric fields are induced in the ionosphere owing to the interaction of the solar wind with the Earth's magnetic field and ionosphere. At *F* region altitudes the collisional effects on ions and electrons are weak for both species, and the ion and electrons are therefore $\mathbf{E} \times \mathbf{B}$ drifting along with the same velocity. At lower altitudes in the *E* region the ion motion is strongly retarded owing to collisions so that ions are no longer effectively $\mathbf{E} \times \mathbf{B}$ drifting but rather moving under the influence of the electric field (and collisions) only. The result is that electrons are streaming through the ion gas. Applying the fluid, kinetic, and nonlinear fluid approximations to this system, *Farley* [1963], *Buneman* [1963], and *Sudan* [1983] showed that the streaming of the electron gas relative to the ion gas in the geomagnetic field results in excitation of a plasma instability, the two-stream instability, if the relative velocity of electrons and ions exceeds the ion acoustic velocity in the plasma. In the approximations used the phase velocity of the two-stream instability plasma waves equals the component of the electron drift velocity on the direction of wave propagation. The actual detailed relationship between the phase velocity of these plasma waves and the electron drift velocity has since been a

subject of intense interest [*St.-Maurice and Hamza*, 2001; *St.-Maurice and Kissack*, 2000; *Hamza and St.-Maurice*, 1993; *Robinson and Honary*, 1990; *Farley and Providakes*, 1989; *St.-Maurice*, 1987; *Robinson*, 1986; *Sudan*, 1983; *Keskinen et al.*, 1979]. The interest arose partly because this relationship depends on the detailed physics of the plasma instability and partly because the phase velocity of the waves can be observed from the ground using radar technique. In effect, the plasma instability made it possible to experimentally observe ionospheric electric fields from the ground. Such measurements can be used to study how a stellar wind interacts with a magnetized planet with an ionosphere.

[3] Experimental evidence supported the finding that useful electron drift velocities could be derived from coherent radar observations of ionospheric plasma waves [*Foster and Erickson*, 2000; *Nielsen and Whitehead*, 1983; *Cahill et al.*, 1978; *Greenwald*, 1977]. However, it also became evident that the possible phase velocities of the plasma waves were limited in magnitude to a value near the ion acoustic velocity [*del Pozo et al.*, 1993; *Kofman and Nielsen*, 1990; *Haldoupis and Schlegel*, 1990; *Nielsen et al.*, 1983; *Nielsen and Schlegel*, 1983]. This meant that the velocity magnitudes, derived for large velocities, became somewhat underestimated, if the estimates were derived directly from the radar measurements without taking into account the limitation of the phase velocities [*Nielsen and Schlegel*, 1985]. Experimentally, a connection was established between the presence of plasma

waves and an increase of the electron temperature in the *E* region. Schlegel and St.-Maurice [1981] found the electron temperature to be enhanced in the altitude range of the ionosphere where two-stream waves were excited. The larger the electron flow speed, the larger the increase of the electron temperature, and thus an increase of the ion acoustic velocity with flow speed was inferred [Jones *et al.*, 1991]. Chen *et al.* [1995] examined the relationship between the variations of the phase velocity and the ion acoustic velocity for increasing electron temperature in the *E* region. They demonstrated that the maximum phase velocity was increasing with increasing electron temperature, albeit not as strongly as was the simultaneous increase in the ion acoustic velocity. Thus they found the ratio of maximum phase velocity to ion acoustic velocity to decrease with increasing electron temperature. The current experimental result is that the maximum phase velocity of two-stream plasma waves in the ionosphere is limited to be near the ion acoustic velocity and that the ratio of the two parameters is decreasing as the ionospheric electron temperature increases, i.e., when the electron drift speed or ionospheric electric field increases.

[4] To excite the primary two-stream instability in a given direction the electron flow velocity component in that direction must exceed the ion acoustic velocity in the plasma. This means that the instability is only excited inside a certain cone centered on the electron velocity. Outside of this cone there should be no primary two-stream waves. Actually, waves are observed all the way up to 180° from the direction of the electron velocity. The waves propagating in directions nearly perpendicular to the electron drift velocity have phase velocities that are experimentally [Nielsen and Schlegel, 1985] and theoretically [Keskinen *et al.*, 1979] found to the first order to equal the electron flow speed component of the direction of the wave propagation vector.

[5] In this paper a much larger amount of joint observations of plasma waves and of electron drift velocities than have been available previously, are used to investigate the relationship between the wave phase velocities, electron drift speeds, and the ion acoustic velocity in the ionospheric *E* region. For electron drift velocities of $\sim 600 \text{ m s}^{-1}$ and for zero flow angle we find the phase velocities to be ~ 1.2 times the ion acoustic velocity at an altitude of $\sim 105 \text{ km}$. As the flow angle increases to 40° the phase velocity decreases to be equal to the ion acoustic velocity. For still larger flow angles the phase velocity is less than the ion acoustic velocity, until for directions nearly perpendicular to the electron drift velocity the phase velocity equals the component of the electron drift velocity on these directions. For electron drift velocities of $\sim 1600 \text{ m s}^{-1}$ and for zero flow angle we find the phase velocities to be ~ 1.05 times the ion acoustic velocity; the rest of the pattern for these larger velocities is similar to the pattern for the smaller electron drift velocities. Using this pattern of the observed line-of-sight velocities, we demonstrate that an estimate of the actual electron drift velocity can be obtained which is an improvement over the estimate obtained when it is assumed that all line-of-sight velocities equal the component of the electron drift velocity on the line of sight.

2. Experiments

[6] The line-of-sight velocities (or Doppler velocities) of the ionospheric plasma waves were measured with the ground-based coherent VHF radar system Scandinavian Twin Auroral Radar Experiment (STARE) [Nielsen *et al.*, 1999]. The radar system consists of two stations. From each station, back scatter intensity and Doppler velocity measurements are made as a function of azimuth and range across northern Scandinavia, also covering the region over European Incoherent Scatter (EISCAT). The STARE observations are continuous with a time resolution of 20 s.

[7] The electron drift velocities and the electron and ion temperatures used to derive the ion acoustic velocity were measured by the ground-based incoherent UHF radar system EISCAT. The radar

measures the ion drift velocity in the *F* region. This is mapped down along a magnetic flux tube to the *E* region. The STARE radar measurements were made in the same flux tube as EISCAT, as determined by the International Geomagnetic Reference Field (IGRF) model. The time resolution of the EISCAT observations was 180 s. The joint radar measurements used in this paper were obtained during the *E* Region Rocket/Radar Instability Study (ERRRIS) campaign [Williams *et al.*, 1990; Pfaff *et al.*, 1992].

3. Observations

[8] All the drift velocities measured by EISCAT, for which STARE measurements are available (from one station or from both), are shown in Figure 1 as imagined arrows, each starting in the origin of the geographic coordinate system and ending in one of the small open circles.

[9] All the measurements were made in the same region over Tromsø, defined by the EISCAT system and the CP-1 common observation program. Thus the directions from this common region to the STARE radar stations define the STARE data to be used in the comparison to EISCAT measurements. These directions are marked by dashed arrows in Figure 1. There is a total of 1334 joint STARE/EISCAT measurements of drift velocity and line-of-sight velocity. Note the good coverage in flow angles and drift speeds. The coverage and amount of data are far exceeding what were used in earlier investigations.

[10] In the data analysis the drift velocities used are the velocities measured by EISCAT, and the flow angles of the STARE measurements are the angle between the drift velocity and the line of sight of the STARE radars for the common observation region. The line-of-sight velocities referred to in the following are all STARE measurements.

[11] In order to obtain a first overview of the relationship between the observed STARE line-of-sight velocities and the electron flow velocities, the line-of-sight velocities are binned in intervals of flow speed and flow angle, as determined from the EISCAT observations. A separate analysis for flow angle $\theta < 90^\circ$ and for flow angles $\theta > 90^\circ$ did not reveal any statistically significant differences. To improve on the statistics it was therefore decided to fold observations for all flow angles in the interval $0^\circ < \theta < 180^\circ$ into a flow angle interval of $0^\circ < \theta < 90^\circ$. The line-of-sight velocity surface is shown in Figure 2a, where the observed Doppler velocities are plotted as a function of the flow angle from 0° to 90° and flow speeds from 0 up to 1200 m s^{-1} , where good coverage is available for all flow angles.

[12] The Doppler velocity is seen to increase with increasing flow speed for all flow angles and to increase with decreasing flow angle for all drift speeds. This results in a minimum line-of-sight velocity for 90° flow angle and minimum flow speed, and in a maximum line-of-sight velocity for zero flow angle and maximum flow speed. In Figure 2b is shown the surface representing the difference (Δ) between the component of the electron drift velocity on the direction of STARE measurements and the STARE line-of-sight measurements, as a function of flow angle and flow speed. Δ is increasing with increasing flow speed and is also increasing with decreasing flow angle. Δ is largest for large flow speeds and small flow angles.

[13] In Figure 3 the STARE observations are displayed in a different quantitative format. For each of several drift speed intervals ($300\text{--}500 \text{ m s}^{-1}$, $400\text{--}600 \text{ m s}^{-1}$, etc. up to $1500\text{--}1700 \text{ m s}^{-1}$) the line-of-sight velocities are binned in 10° wide steps in flow angle, covering the flow angle interval $0^\circ\text{--}180^\circ$ but with all flow angles folded into the interval from 0° to 90° . This is equivalent to displaying the numerical values of the mean line-of-sight velocities. The mean flow speed observed by EISCAT in each drift speed interval is shown in parentheses. The mean drift velocity is displayed as a solid headed arrow. The half circle with a diameter equal to the flow speed represents the contour of the

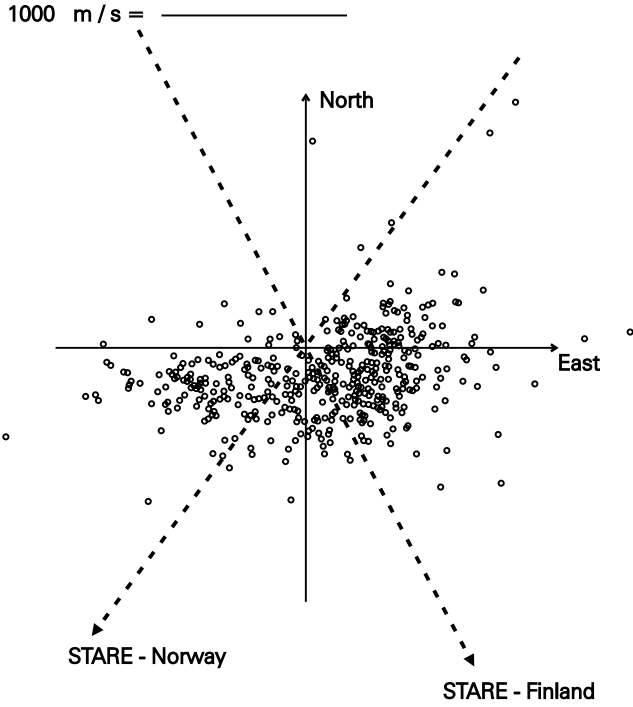


Figure 1. Electron drift velocities observed with European Incoherent Scatter (EISCAT) for which simultaneous Scandinavian Twin Auroral Radar Experiment (STARE) measurements are available. The velocities are represented by imagined arrows, starting in origo and ending in the small circles. The velocities are plotted in geographic coordinates. The dashed lines with the solid arrow heads point toward the STARE radar stations located near Trondheim in Norway and near Hankasalmi in Finland, respectively.

components of the electron drift velocity projected on the flow angle. The mean values of the binned data, i.e., the mean line-of-sight velocities, are plotted as a function of the mean flow angle and are marked by crosses. For each angular interval the standard deviation on the mean line-of-sight velocity is plotted as a solid line centered on the mean velocity. Each of these mean values of the STARE line-of-sight velocities are associated with a mean ion acoustic velocity derived from simultaneous EISCAT electron and ion temperature measurements, T_e and T_i , in 105-km altitude, using the isothermal long wave limit of the ion acoustic velocity,

$$V_{iac} = \sqrt{\frac{k_B(T_e + T_i)}{m}}, \quad (1)$$

where “ k_B ” is Boltzman’s constant and “ m ” is the mean ion density in the plasma (here m equals 32 atomic units). The mean values of the binned ion acoustic velocities are plotted as a function of the mean flow angle and are marked by circles. The average value of all the mean ion acoustic velocities is calculated, and the radius of the dashed circle section equals this average value. The observed average ion acoustic velocities are close to nominal ion acoustic velocity and the limiting line-of-sight velocity of *Nielsen and Schlegel* [1985],

$$V_{ph} = 300.0 + 0.00011(V_e^2). \quad (2)$$

[14] The dashed line marks the limit of the cone in which the two-stream instability can be excited, and this limit is calculated for the observed mean electron drift velocity and mean ion acoustic velocity. Data points inside this cone are the line-of-sight velocities

associated with the primary two-stream instability; data points outside the cone are associated with the secondary wave activity.

[15] The solid curve in each of the plots in Figure 3 represents a fit to the line-of-sight (LOS) velocities inside the two-stream instability cone. The curve is given by

$$V_{LOS} = V_{iac} \left[\frac{\cos\theta}{\cos\theta_o} \right]^\alpha. \quad (3)$$

Attempts of least squares fit to determine α and θ_o were made, but the minimum is quite wide, precluding a firm determination of the two parameters. However, the observations are consistent with a θ_o close to 40° , and the value of α tends to decrease (from 0.8 to 0.2)

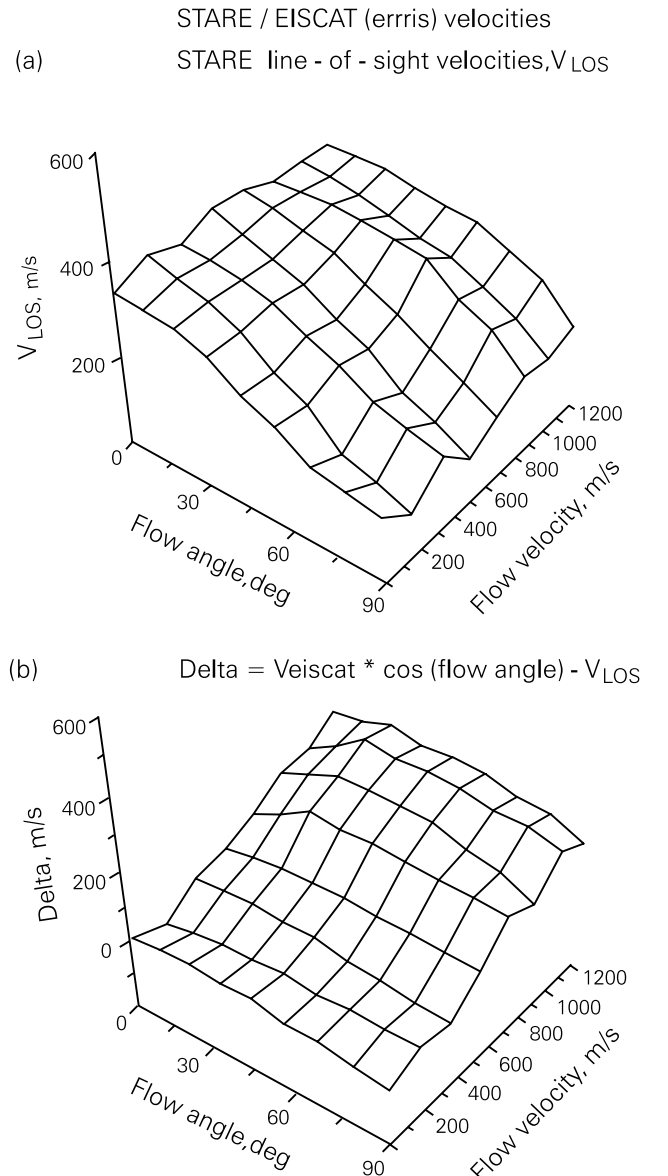


Figure 2. (a) Surface of observed line-of-sight velocities as a function of drift speed and flow angle. The velocity increases with drift speed and with decreasing flow angle. (b) Surface of the difference between the component of the electron drift velocity on flow angle and the observed line-of-sight velocity for that flow angle, versus drift speed and flow angle. The difference increases with drift speed and with decreasing flow angle.

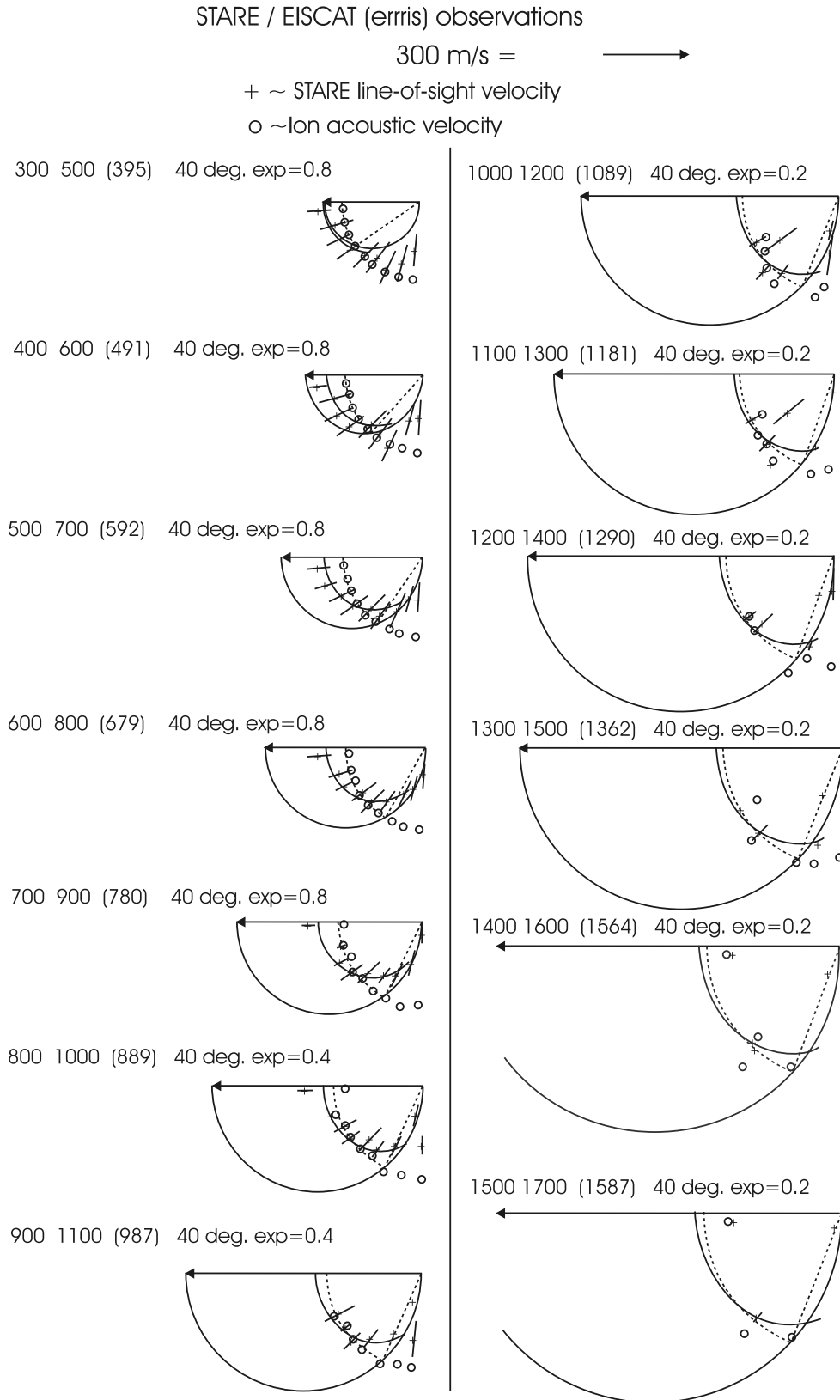


Figure 3. Mean STARE line-of-sight velocities for several different drift speed intervals plotted versus flow angle (the angle between the electron velocity and the radar line of sight). The velocities are averaged over 200 m s^{-1} drift speed intervals and over 10° flow angle intervals. The start and end drift speeds are shown in each panel together with the mean drift speed (in parentheses). The solid curve is a fit to the line-of-sight velocities. For each mean line-of-sight velocity is also shown the standard deviation on the mean and also the simultaneously observed mean ion acoustic velocity. The dashed curves (circle section) mark the observed average ion acoustic speed, and the dashed lines mark the width of the two-stream instability cone.

as the drift speed increases from 400 to 1600 m s⁻¹. The curves should rather be seen as a guide to reveal the variation of the line-of-sight velocities with increasing flow angle. For small drift speeds the line-of-sight velocity is larger than the V_{iac} for small flow angles and is smaller at large flow angles near the sides of the instability cone ($\alpha = 0.8$). At large drift speeds the line-of-sight velocity shows less variation with flow angle ($\alpha = 0.2$). For $\theta = 0$ the ratio V_{LOS}/V_{iac} decreases from a value of 1.2 for low velocities ($\alpha = 0.8$) to 1.05 for large velocities ($\alpha = 0.2$). Thus the maximum line-of-sight velocity is larger than the ion acoustic velocity, but the value approaches the ion acoustic velocity for increasing electron flow speeds.

[16] A separate analysis of the line of sight for large flow angles ($60^\circ < \theta < 120^\circ$) was made in order to determine the variations of the line of sight in directions nearly perpendicular to the electron drift velocity. In Figure 4 is shown the line-of-sight velocities binned in 4° wide flow angle intervals in the range from -30° to $+30^\circ$ around the perpendicular direction, corresponding to the flow angle interval given above. The mean value for positive and negative angles is marked by a circular symbol.

[17] The curve is determined by the variation of the component of the observed mean electron drift velocity on the directions determined by these flow angles. The fit of the curve to the data points supports the view that the line-of-sight velocities at these large flow angles are equal to the electron drift velocity component. Some key parameter values are listed in Table 1.

4. Discussion

[18] The line-of-sight velocities at large flow angles ($\sim 60^\circ < \theta < \sim 120^\circ$), outside the two-stream instability cone, are consistent with the notion that they are equal to the component of the electron drift velocity projected on that flow angle. Thus the line of sight for 90° flow angle is consistent with a value of zero.

[19] The observed ion acoustic velocities are consistent with the values of the ‘‘limiting line-of-sight’’ velocity, V_{ph} , in (2). The limiting line-of-sight velocity, or the ion acoustic velocity,

STARE / EISCAT (errris) observations

EISCAT velocities
300 1700

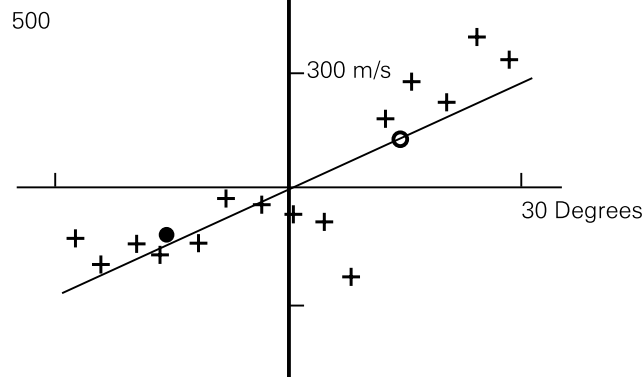


Figure 4. STARE line-of-sight velocities binned in 4° wide angular intervals between 120° and 60° flow angle (corresponding to -30° and $+30^\circ$ in the plot) are shown as a function of the line-of-sight deviation from the direction perpendicular to the electron drift velocity. The circle (dot) is the mean of the data from 0° to $+30^\circ$ (-30° to 0°). The curve traces the component of the 550 m s⁻¹ mean electron drift on the line of sight. The good fit of the curve to the measurements indicates that the mean phase velocity at 90° flow angle is zero.

Table 1. Parameter Values for Low and High Electron Drift Speeds^a

V_o	V_{LOS}	V_{isc}	V_{pm}	V_{LOS}/V_{isc}
600	410	335	340	1.2
1600	610	575	585	1.05

^a V_o is electron drift speed, EISCAT. V_{LOS} is line-of-sight velocity, STARE. V_{isc} is ion acoustic velocity at 105-km altitude (equation (1)). V_{pm} is limiting phase velocity (equation (2)).

increases from 310 to 585 m s⁻¹ when the electron drift speed increases from 300 to 1600 m s⁻¹. The line-of-sight velocity is equal to the ion acoustic velocity at a flow angle of 40° , independent of the electron drift speed. The variation of the line-of-sight velocity for $0^\circ < \theta < 60^\circ$ is given by (3), with α decreasing from 0.8 to 0.2 for increasing electron drift speed. The extrapolated line-of-sight velocity for zero flow angle (using equation(3)) yields 410 m s⁻¹ for $V_e = 600$ m s⁻¹, and for $V_e = 1600$ m s⁻¹ the line-of-sight velocity is 610 m s⁻¹ (for a more detailed quantitative comparison the altitude of the backscattering region would have to be known, but it is not measured in this experiment).

[20] For a low electron drift speed of $V_e \sim 350$ m s⁻¹, which is close to the ion acoustic velocity in the plasma, the line-of-sight velocities are close to the value of the component of the drift velocity on the line of sight. For drift speed increases up to 800 m s⁻¹ the line-of-sight velocity for waves inside the two-stream cone is decreasing with increasing flow angle. For flow angles less than 40° the line-of-sight velocities are larger than the ion acoustic velocity. For larger flow angles the limiting velocity tends to be smaller than the ion acoustic velocity (this strong dependence on θ will be discussed below to be a possible consequence of secondary wave activity in the backscattering volume). Within this framework the line-of-sight phase velocity at near-zero flow angles is larger than the ion acoustic velocity in 105-km altitude.

[21] For drift speeds larger than ~ 1000 m s⁻¹ the line-of-sight velocity of two-stream waves stays closer to the ion acoustic velocity over the flow angle interval, than does that for smaller drift speeds. For these larger drift speeds we do not have as good a data coverage as that for smaller drift speeds, especially at small flow angles. This increases the uncertainty on the parameter α , but a value between 0.2 and 0.4 is realistic.

[22] From Figure 3 it can be seen that for small drift speeds the line-of-sight velocity for zero flow angle is $\sim 20\%$ larger than the average ion acoustic velocity, and it decreases to only $\sim 5\%$ for large drift speeds. At $V_e = 600$ m s⁻¹ we have $V_{iac} = 335$ m s⁻¹, and for $V_e = 1600$ m s⁻¹ we have $V_{iac} = 575$ m s⁻¹. The line-of-sight velocity for zero flow angle is a factor ~ 1.2 (~ 1.05) larger than the ion acoustic velocity at 105-km altitude for small (large) drift speeds. The decrease in the V_{LOS}/V_{iac} ratio is qualitatively consistent with the results of *Chen et al.* [1995].

[23] Owing to the dependence of the ion acoustic velocity on altitude, the value of V_{LOS}/V_{iac} is strongly dependent on the altitude of the backscatter layer. The ratio of the line-of-sight to ion acoustic velocity will decrease for increasing electron drift speed, independent of the backscatter altitude. However, the value of the ratio will be >1 or <1 depending on the backscatter altitude. *Chen et al.* [1995], also analyzing STARE and EISCAT measurements, showed that the ratio between the phase velocity and the ion acoustic velocity was close to 1 for small drift speeds and decreased with increasing plasma electron temperature (increasing electron drift speeds) to a value of 0.8. However, these authors used plasma temperature measurements averaged over 106- to 116-km altitude, where the ion acoustic velocities are larger than those at 105 km so far considered in this work. For small velocities they used $V_{iac} = \sim 400$ (335) m s⁻¹, and for $V_e = 1600$ m s⁻¹ they used $V_{iac} = 780$ (575) m s⁻¹, where the number in parentheses is the value used in this work. Similarly, *Kofman and Nielsen* [1990] found that the line-of-sight velocities tend to be lower than or

limited by the ion acoustic velocity, derived from temperature measurements in 112-km altitude. Since we have no direct information on the actual backscatter altitude, we can only conclude that an assumed backscatter altitude near 105 km yields good agreement between the measurements and earlier results. For an assumed backscatter altitude near 110 km and higher, the ratio of line-of-sight and ion acoustic velocities is close to 1 for small velocities and decreases to a value of 0.8 for large velocities.

[24] However, this subject is intricate, and there are several more factors that must be considered with regard to the ratio of line-of-sight velocity and ion acoustic velocity. The ion acoustic velocity used in this discussion was calculated under assumption of isothermal electrons and ions equation (1). While the ions are generally expected to be isothermal, the electrons may be adiabatic [Farley and Providakes, 1989]. If the electrons should be adiabatic, then for low electron and ion temperatures it results in an ion acoustic velocity a factor 1.15 larger than the isothermal case, and for large temperatures it results in a factor 1.25 increase. The ratio of line-of-sight velocity and ion acoustic velocity for our observations would then vary from ~ 1 to ~ 0.8 for drift velocities increasing from 600 to 1600 m s⁻¹. Thus, in the isothermal case the ratio $V_{\text{LOS}}/V_{\text{iac}} = 1.2(1.05)$ for small (large) drift velocities, while in the case of adiabatic electrons, $V_{\text{LOS}}/V_{\text{iac}} = 1.0(0.8)$ for small (large) velocities. The only way to distinguish between these possibilities would be to obtain measurements of the electron specific heat ratio. Actually, *St.-Maurice and Kissack* [2000] predicted that inelastic collisions with neutrals are too frequent to allow for adiabatic electrons. The ratio may also be influenced by the Pedersen conductivity instability discussed by *Robinson* [1998] and by *Dimant and Sudan* [1997], which may decrease the threshold speed at negative flow angles and increase it at positive flow angles. The situation may be further complicated: The altitude of the largest-amplitude irregularities may be changing as the electric field strength increases. Thus there are many reasons to be very careful when explaining changes in the line-of-sight velocities with respect to the ion acoustic speed.

[25] It must be noted that the theory of the plasma instability predicts the variations of the wave phase velocity, while with the STARE system a line-of-sight velocity, or a Doppler velocity, is measured. The relationship of this Doppler velocity to the phase velocity is determined by the form of the power spectrum of the radar signal backscattered from the plasma waves and by the technique by which the Doppler velocity is measured.

[26] In the STARE system the line-of-sight velocity is measured using a double-pulse technique. Two pulses with a time separation of 300 μs are transmitted, and the phase difference between the received pulses is measured. From this difference a measure of the wave phase velocity in the line of sight is deduced [see, e.g., *Nielsen*, 1989]. We assume that the theoretical phase velocity is related to the mean frequency of the backscattered power spectrum. If the backscattered power spectrum is $S(f)$, then the mean frequency is

$$\langle f \rangle = \int f S(f) df. \quad (4)$$

However, using a double-pulse technique, one measures not $\langle f \rangle$ but f_o given by

$$\int \sin[2\pi T(f - f_o)] S(f) df = 0. \quad (5)$$

[27] One can show that for a symmetric spectrum or for a narrow spectrum, $f_o = \langle f \rangle$. In practice, we find that the phase velocity measured using the double-pulse technique is typically less than the mean frequency of the power spectrum. This differ-

ence is caused by a slight asymmetry of the power spectra, which typically have a tail extending from the peak power toward lower frequencies [*Nielsen et al.*, 1984]. Thus, owing to use of the double-pulse technique, a detailed comparison of the measured “phase velocities” with the ion acoustic velocity is further complicated.

[28] Discussing the limitation of the phase velocity inside the instability cone, it must be considered that the limit is found to vary with flow angle (equation (3)). In the framework of the previous paragraph, it is clear that this behavior may be caused by a flow angle dependence of the power spectrum. If the spectrum is becoming increasingly asymmetric with a tail toward lower frequencies as the flow angle increases, then the observed phase velocity variation could be explained. Such a variation of the spectrum has been observed [*Haldoupis et al.*, 1984]. The total power spectrum was proposed to be composed by two spectra: one narrow spectrum peaking near the ion acoustic velocity arising from the primary two-stream instability waves and one broad spectrum centered at zero frequency arising from secondary waves excited in the primary waves. *Andre* [1980] showed that the backscatter intensity from primary waves exceeds that for secondary waves by 5–20 dB for increasing velocity magnitude. Thus, for small flow angles, when the line-of-sight velocity is largest, the primary waves dominate the total spectrum. As the flow angle increases, the power of the signal backscattered from the primary waves decreases, and the signal backscattered from the secondaries increases in importance, resulting in an increasingly asymmetric total spectrum as the flow angle decreases. This could be part of the reason for the observed decrease of the limiting phase velocity relative to the ion acoustic velocity as the flow angle increases.

[29] *Nielsen and Schlegel* [1985] implemented a procedure for correcting the STARE line-of-sight velocities to better approximate the component of the electron drift velocity along the line of sight. This allowed for an improved estimate of the electron drift velocity from the STARE observations. This same procedure has here been applied to the new observations presented in this work. Since the procedure was developed using another data set, this is a significant new test of the general validity of the procedure. The result of the test is shown in Figure 5 (see figure caption for data format), where electron drift velocities in several magnitudes and angular intervals are compared.

[30] The sorting of data is done against EISCAT velocity measurements. Overall, the agreement between the EISCAT measured drift velocity and the improved estimate derived from the STARE measurements is satisfactory, even though there are some cases of deviations between the two data sets, both in direction and magnitude of the velocities. The reason it is possible to derive a realistic estimate of the electron drift velocity from STARE measurements is that the increase of the line-of-sight velocity with drift speed is relatively large (it increases from ~ 310 m s⁻¹ for $V_e = 300$ m s⁻¹ to ~ 585 m s⁻¹ for $V_e = 1600$ m s⁻¹; see Table 1). The backscattered signal is influenced not only by the electron drift velocity but also by the neutral wind, the ion drift speed, the mean ion mass, the asymmetry of the power spectrum, and the altitude of the backscatter region. The scatter is caused by real variations in the backscatter region of these parameters, which are not measured in the current experimental setup, so the line-of-sight measurements cannot be corrected for these variations. Nevertheless, Figure 5 shows that the corrected velocities are generally an improvement over the estimate obtained simply by equating the measured line-of-sight velocity with the component of the drift velocity on the line of sight. If the statistical fluctuation of the measurements is large, it causes large scatter in the recovered velocities. This is so because the Doppler velocities increase weakly with electron velocity magnitude. It is concluded that time-averaged measurements with corresponding low statistical error can be recovered with better accuracy.

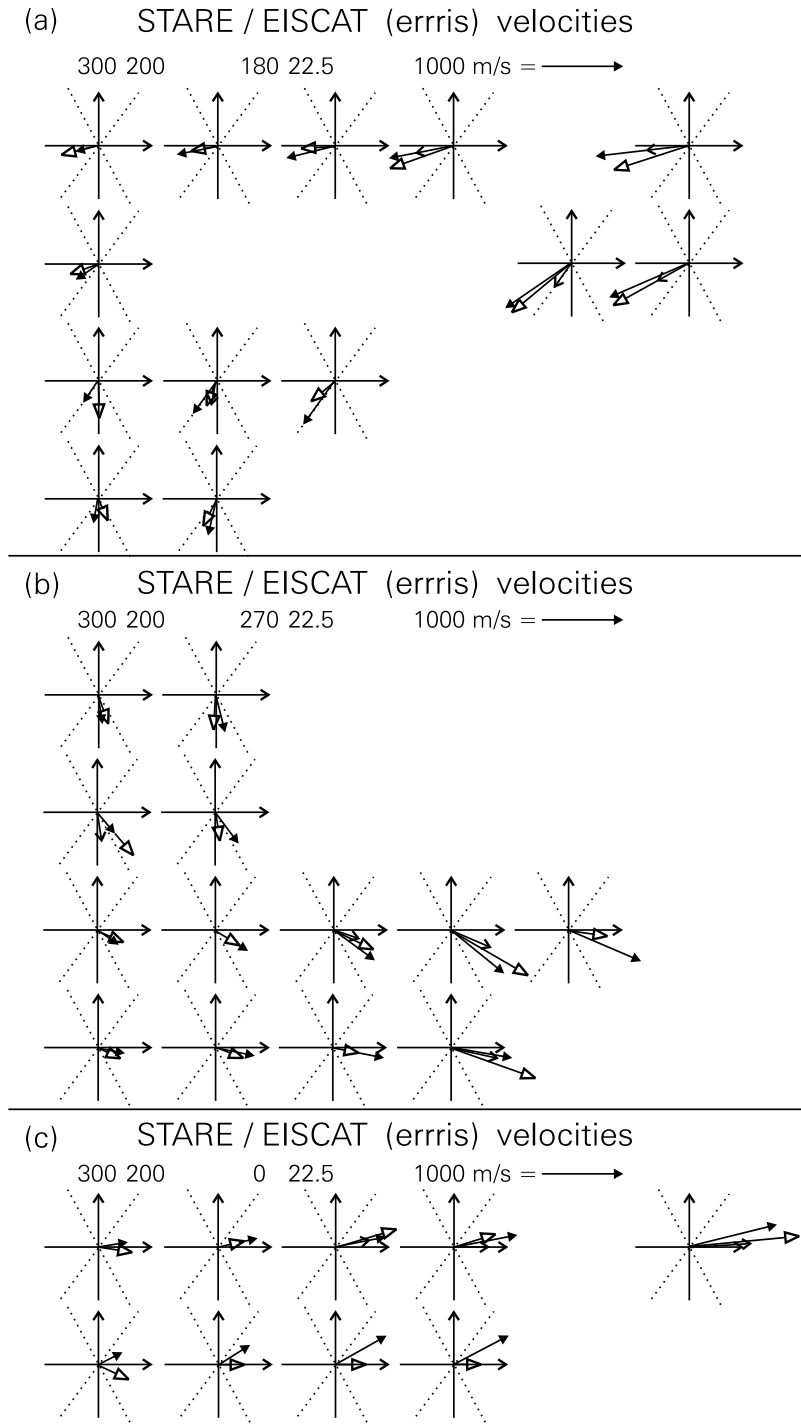


Figure 5. (a–c) Drift velocity estimates determined from STARE Doppler velocity observations for several drift speed and flow angle intervals in a quadrant of the geographic coordinate system. The sorting of velocities is done against EISCAT velocity measurements. For each interval the east-west and north-south geographic coordinate axes are plotted (solid lines with open arrow), as well as the line of sight from the two STARE stations (dashed lines). Furthermore, three arrows representing the three drift velocity estimates are plotted: EISCAT (solid arrow), STARE-corrected (closed arrow), and STARE-irregularity (open arrow). If the open arrow is not visible, it means it has been overwritten by the closed arrow; that is, the STARE-corrected value is in that case closely similar to the STARE-irregularity value. The data are arranged so that the drift speed increases toward the right in each row and the flow angle increases downward in each column. The drift speed intervals are the same in Figures 5a–5c. In the leftmost column, drift speed ranges from 300 to 500 m s^{-1} ; in the next column, drift speed ranges from 500 to 700 m s^{-1} , etc. The flow angle coverage is different for each panel. For Figure 5a (third quadrant) the interval in the topmost row ranges from 180° to 202.5° ; in the next row the interval ranges from 202.5° to 225° , etc. For Figure 5b (fourth quadrant) the interval in the topmost row ranges from 270° to 292.5° ; in the next row the interval ranges from 292.5° to 315° , etc. For Figure 5c (first quadrant) the interval in the topmost row ranges from 0° to 22.5° ; in the next row the interval ranges from 22.5° to 45° .

[31] We have considered to what extent the electron drift velocity, in magnitude and direction, can be derived from the STARE measurements, and it is clear that statistical fluctuations in several parameters in the backscatter volume introduce uncertainties. It is often not only the absolute electron drift velocity that is required for geophysical studies, but rather the relative variations of the drift velocity estimate. For example, *Allan et al.* [1982] studied a geomagnetic pulsation event where the pulsation amplitude was $\leq 100 \text{ m s}^{-1}$. Even though the velocity pulsation amplitude was so small, it was nevertheless clearly observed and could be followed for several hours. For this event it appears that there was little fluctuation in the values of the parameters (listed above) which influence the electron drift velocity estimates. The experience is that even though the DC component of the velocity may be uncertain, small fluctuations relative to the DC component can be reproduced quite accurately using STARE data. It is therefore also of interest to use EISCAT observations to examine to what extent the variations of the estimated velocity around a DC velocity value are a good approximation of the actual drift velocity variations. This is best done using observations during geomagnetic pulsation events, but this requires a better time resolution of EISCAT measurements than is possible with the current system. It is to be expected that a technical update of the EISCAT system during the summer of 2001 (M. Rietveld, private communication, 2001) will enable the incoherent radar system to obtain velocity data with sufficient time resolution and statistical accuracy to make it possible to use such measurements to evaluate how accurate relative velocity variations can be determined using STARE observations.

[32] The results of the comparison of the coherent radar (STARE) measurements of Doppler velocities of $\sim 1 \text{ m}$ plasma waves in the ionospheric E region to ion (electron) drift velocity measurements by an incoherent radar (EISCAT) are as follows:

1. The line-of-sight velocities observed with a 140-MHz coherent radar are limited to values near the ion acoustic velocity.

2. The maximum line-of-sight velocity is observed for zero flow angle and has a value that is a factor ~ 1.2 (1.05) times larger than the ion acoustic velocity for electron flow speeds of ~ 600 (1600 m s^{-1}).

3. The ratio of the maximum line-of-sight velocity to the ion acoustic velocity is decreasing from 1.2 to 1.05 when the electron drift speed increases from 600 to 1600 m s^{-1} .

4. The line-of-sight radar velocity variation with flow angle is described as $\cos^\alpha \theta$, where $\alpha \sim 0.8$ for small velocities ($\sim 600 \text{ m s}^{-1}$) and $\alpha \sim 0.2$ for large velocities ($\sim 1600 \text{ m s}^{-1}$).

5. Waves propagating perpendicular to the electron drift velocity have zero phase velocity.

6. The line-of-sight velocity observed with a 140-MHz coherent radar is increasing as a function of increasing electron flow speed and of decreasing flow angle.

7. The line-of-sight velocities are decreasing relative to the ion acoustic velocity with increasing flow angle, possibly owing to contamination of the two-stream backscattered power spectrum by secondary waves, and because the velocity measurements are made using a double-pulse technique.

8. The line-of-sight velocity at $\sim 40^\circ$ flow angle is a good match to the nominal ion acoustic speed.

[33] Observations with the current STARE system include measurements of the spectrum of the backscattered signal. The spectral data allow a more detailed analysis of the backscatter process than does the use of only line-of-sight velocities obtained by the double-pulse technique. We plan to exploit this new capability in a new joint STARE/EISCAT campaign.

[34] **Acknowledgments.** The STARE system is operated jointly by the Max Planck Institute for Aeronomie, Germany, and by the Finnish Meteorological Institute, Finland, in cooperation with SINTEF, University of Trondheim, Norway. EISCAT is an international facility supported by

Finland, France, Germany, Norway, Sweden, and the UK. We are indebted to the UK Particle Physics and Astronomy Research Council for the support for one of us (C. F. d. P.) during the time this work was completed.

[35] Michel Blanc thanks Terry Robinson and Jean-Pierre St.-Maurice for their assistance in evaluating this paper.

References

- Allan, W., E. M. Poulter, and E. Nielsen, STARE observations of a Pc5 pulsation with large azimuth wave number, *J. Geophys. Res.*, **87**, 6163, 1982.
- Andre, D., Radarmessungen von Plasmawellen in der Polaren Ionosphäre, thesis, George-August-Universitaet, Goettingen, Germany, 1980.
- Buneman, O., Excitation of field aligned sound waves by electron streams, *Phys. Res. Lett.*, **10**, 285, 1963.
- Cahill, L. J., Jr., R. A. Greenwald, and E. Nielsen, Auroral radar and rocket double-probe observations of electric field across the Harang discontinuity, *Geophys. Res. Lett.*, **5**, 687, 1978.
- Chen, P.-R., L. Yi, and E. Nielsen, Variations of the mean phase velocity of 1-m ionospheric plasma waves with the plasma electron temperature, *J. Geophys. Res.*, **100**, 1647, 1995.
- del Pozo, C. F., J. C. Foster, and J.-P. St.-Maurice, Dual-mode E region plasma wave observations from Millstone Hill, *J. Geophys. Res.*, **98**, 6013, 1993.
- Dimant, Y. S., and R. N. Sudan, Physical nature of a new cross-field current-driven instability in the lower ionosphere, *J. Geophys. Res.*, **102**, 2551, 1997.
- Farley, D. T., A plasma instability resulting in field-aligned irregularities in the ionosphere, *J. Geophys. Res.*, **68**, 6083, 1963.
- Farley, D. T., and J. Providakes, The variation with T_e and T_i of the velocity of unstable ionospheric two-stream waves, *J. Geophys. Res.*, **94**, 15,415, 1989.
- Foster, J. C., and P. J. Erickson, Simultaneous observations of E-region coherent backscatter and electric field amplitude at F-region heights with the Millstone Hill UHF radar, *Geophys. Res. Lett.*, **27**, 3177, 2000.
- Greenwald, R. A., Recent advances in the use of radar auroral backscatter to measure ionospheric electric fields, in *Dynamical and Chemical Coupling*, edited by B. Grandal and J. A. Holtet, pp. 291–312, D. Reidel, Norwell, Mass., 1977.
- Haldoupis, C., and K. Schlegel, Direct comparison of 1-m irregularity phase velocities and ion acoustic speeds in the auroral E region ionosphere, *J. Geophys. Res.*, **95**, 18,989, 1990.
- Haldoupis, C. I., E. Nielsen, and H. M. Ierkec, STARE Doppler spectral studies of westward electrojet radar aurora, *Planet. Space Sci.*, **32**(10), 1291, 1984.
- Hamza, A.M., and J.-P. St.-Maurice, A self-consistent fully turbulent theory of auroral E region irregularities, *J. Geophys. Res.*, **98**, 11,601, 1993.
- Jones, B., P. J. S. Williams, K. Schlegel, T. Robinson, and I. Haggstrom, Interpretation of enhanced electron temperatures measured in the auroral E-region during ERRRIS campaign, *Ann. Geophys.*, **9**, 55, 1991.
- Keskinen, M. J., R. N. Sudan, and R. L. Ferch, Temporal and spatial power spectrum studies of numerical simulations of type II gradient drift instabilities in the equatorial electrojet, *J. Geophys. Res.*, **84**, 1419, 1979.
- Kofman, W., and E. Nielsen, STARE and EISCAT measurements: Evidence for the limitation of STARE Doppler velocity observations by the acoustic velocity, *J. Geophys. Res.*, **95**, 19,131, 1990.
- Nielsen, E., Coherent radar technique, in *World Ionosphere/Thermosphere Study: WITS Handbook*, vol. 2, edited by C. H. Liu, pp. 285–318, Sci. Comm. on Sol. Terr. Phys., Univ. of Ill., Urbana, 1989.
- Nielsen, E., and K. Schlegel, A first comparison of STARE and EISCAT electron drift velocity measurements, *J. Geophys. Res.*, **88**, 5745, 1983.
- Nielsen, E., and K. Schlegel, Coherent radar Doppler measurements and their relationship to the ionospheric electron drift velocity, *J. Geophys. Res.*, **90**, 3498, 1985.
- Nielsen, E., and J. D. Whitehead, Radar auroral observations and ionospheric electric fields, *Adv. Space Phys.*, **2**(131), 1983.
- Nielsen, E., J. D. Whitehead, L. A. Hedberg, and T. B. Jones, A test for the cosine relationship using three-radar velocity measurements, *Radio Sci.*, **18**, 230, 1983.
- Nielsen, E., C. I. Haldoupis, B. G. Fejer, and H. M. Ierkec, Dependence of auroral power spectra variations upon electron drift velocity in the eastward electrojet, *J. Geophys. Res.*, **89**, 253, 1984.
- Nielsen, E., M. Bruns, I. Pardowitz, H. Perplies, L. Bemann, P. Janhunen, and A. Huuskonen, STARE: Observations of a field-aligned line current, *Geophys. Res. Lett.*, **26**, 21, 1999.
- Pfaff, R. F., et al., The E-region rocket/radar instability study (ERRRIS): Scientific objectives and campaign overview, *J. Atmos. Terr. Phys.*, **54**, 779, 1992.
- Robinson, T. R., Towards a self-consistent nonlinear theory of radar auroral back scatter, *J. Atmos. Terr. Phys.*, **48**, 416, 1986.

- Robinson, T. R., The Effects of small scale field aligned irregularities on *E*-region conductivities: Implication for electron thermal processes, *Adv. Space Res.*, 22(9), 1357, 1998.
- Robinson, T. R., and F. Honary, A resonance broadening kinetic theory of the modified two-stream instability: Implications for radar auroral backscatter experiments, *J. Geophys. Res.*, 95, 1073, 1990.
- Schlegel, K., and J.-P. St.-Maurice, Anomalous heating of the polar *E* region by unstable plasma waves, *J. Geophys. Res.*, 86, 1447, 1981.
- St.-Maurice, J.-P., A unified theory of anomalous resistivity and Joule heating effects in the presence of *E*-region irregularities, *J. Geophys. Res.*, 92, 4533, 1987.
- St.-Maurice, J.-P., and A. M. Hamza, A new nonlinear approach to the theory of *E* region irregularities, *J. Geophys. Res.*, 106, 1751, 2001.
- St.-Maurice, J.-P., and R. S. Kissack, The role played by thermal feedback in heated Farley-Buneman waves at high latitudes, *Ann. Geophys.*, 98, 532, 2000.
- Sudan, R. N., Unified theory of type I and type II irregularities in the equatorial electrojet, *J. Geophys. Res.*, 88, 4853, 1983.
- Williams, P. J. S., G. O. L. Jones, H. Opgenoorth, and I. Haggstrom, High-resolution measurements of magnetospheric electric fields, *J. Atmos. Terr. Phys.*, 52, 439, 1990.
-
- C. F. del Pozo, Communications Research Centre, Faculty of Applied Sciences, Lancaster University, Lancaster LA1 4YW, UK. (c.del.pozo@lancaster.ac.uk)
- E. Nielsen, Max-Planck-Institut für Aeronomie, Max-Planck-Strasse 2, D-37191 Katlenburg-Lindau, Germany. (nielsen@linmpi.mpg.de)
- P. J. S. Williams, Adran Ffiseg, Prifysgol Cymru, Aberystwyth SY23 3BZ, UK. (pjw@aber.ac.uk)